Water injection in a microgasturbine – Assessment of the performance using a black box method

Ward De Paepe[a*], Frank Delattin[a], Svend Bram[ab], Jacques De Ruyck[a]

[a]Vrije Universiteit Brussel, Dept. of Mechanical Engineering (MECH), Pleinlaan 2, 1050 Brussel, Belgium

***Corresponding author:** e-mail: wdepaepe@vub.ac.be, Tel: +32-2-6293182, Fax: +32-2-6292865

[b]Erasmushogeschool Brussel

Dept. of Industrial Sciences and Technology (IWT), Nijverheidskaai 170, 1070 Brussel, Belgium

Abstract:

Microturbines offer new perspectives in small-scale heat and power production however their profitability depends strongly on the yearly amount of running hours. The non-continuous heat demand often leads to a reduction in running hours. This paper proposes an alternative by recuperating the lost thermal power through the injection of heated water in the micro Gas Turbine (mGT). Water injection is considered a successful way to increase power and efficiency in industrial gas turbines and similar effects are expected for microturbines. This paper reports on a series of simulations of water injection performed on a Turbec T100 mGT. The goal of this study was to investigate the potential of water injection in the mGT cycle using an adiabatic black box method in the Aspen® process simulation tool. Past experiments with steam injection on the T100 demonstrated the potential of introducing steam/water in the microturbine cycle.

Calculations revealed that the key parameters for maximum heat recuperation are stack and pinch temperature. Simulations showed that most of the exhaust heat can be recovered through injection of heated water after the compressor, resulting in an 18% decrease in fuel consumption and an absolute increase in electrical efficiency of 7%.

Keywords:

Microturbine, water injection, steam injection, black box simulation, thermodynamic simulations.

Nomenclature:

Acronyms

BB	Black Box
CHP	Combined Heat and Power
GB	Grey Box
HAT	Humid Air Turbine
mGT	micro Gas Turbine
mHAT	micro Humid Air Turbine
REVAP®	REgenerative EVAPoration cycle
STIG®	Steam Injected Gas Turbine
TIT	Turbine Inlet Temperature [˚C]
TOT	Turbine Outlet Temperature [˚C]

Symbols

π	Pressure ratio
$\dot{E}x$	Exergy flow [kW]
$\dot{m}$	Mass flow [kg/s]
$\dot{Q}$	Heat flux [kW]
T	Temperature [°C]

Subscripts

HEATER	Heater
dest	Destruction

eff	Efficiency
gain	Flow gaining exergy
COOLER	Cooler
in	Ingoing flow
loss	Flow losing exergy
natgas	Natural gas
out	Outgoing flow
SAT	Saturator

1 Introduction

Microturbines in Combined Heat and Power (CHP) mode are very cost efficient [1, 2]. In literature, a large number of papers concerning the problems of necessary installed power [3, 4] and control strategy (thermal power versus electric power) [5-7] can be found. One of the occurring problems however is the non-continuous heat demand. The changing heat demand will lead to a reduced number of running hours and a less profitable investment [8]. One possible solution for this problem is increasing the electric efficiency of the microturbine. The electric efficiency of gas turbines can be increased by increasing the heat recuperation [9]. Most current research focusses on the improvement of the gas/gas heat recuperation, by improving the efficiency of the recuperator of the micro Gas Turbine (mGT) [10-12]. Improved recuperator efficiency however does not supply a solution for the changing heat demand and does not give any flexibility in changing the heat to power ratio of the microturbine. Recuperating the lost thermal power by introducing water or steam in the microturbine system provides the flexibility needed to make the investment more efficient. The effects of steam injection in a mGT have been simulated [8] and experimentally validated [13] on a Turbec T100 mGT by the authors of this paper. In their review paper, concerning

the topic of humidified gas turbines, Jonsson and Yan [14] showed that the evaporative gas turbine with humidification tower – the so-called Humid Air Turbine (HAT) as proposed by Rao [15] – has the highest efficiency of the mixed air/water gas turbine cycles. A lot of research work has already been performed on the topic of micro Humid Air Turbines (mHAT) [16-19], demonstrating the positive effect of using humid air on microturbine efficiency and increasing the specific work. The off-design behaviour of the mGT has been simulated [20], showing that the mHAT has a more favourable off-design performance than the recuperated mGT. However, due to the absence of an intercooler and the limited amount of available waste exergy, the full performance of an optimized HAT cycle is not entirely reached.

The goal of this paper is to investigate the potential of water injection in an mGT cycle using an adiabatic black box method implemented in the Aspen® process simulation tool. Results of water injection calculations in a T100 Turbec mGT are presented. Past experiments with steam injection in the T100 already showed the potential of introducing steam/water in an mGT cycle [13].

The final goal of this study is to develop a mGT layout that can work as a CHP unit when there is heat demand but that can also switch to water injection mode with higher electrical efficiency when the heat demand drops. By doing so, forced shut down is avoided, resulting in a more profitable investment. Delattin et al. showed the positive effect of combining a CHP with Steam Injected Gas Turbine (STIG®) mode in a mGT on payback time, net present value and internal rate of return [8]. Similar effects are expected when using water injection mode instead of STIG® mode.

2 Approach

Fig. 1 shows a typical recuperated mGT cycle. After entering the compressor (1), the compressed air will enter the recuperator for partial recuperation of the remaining heat in the

exhaust gases (2). In the combustion chamber, natural gas is injected to increase the temperature of the compressed gas up to the maximum Turbine Inlet Temperature (TIT) (3). The hot gases will expand in the turbine, which is connected with a single shaft to the compressor and the high speed electric generator. After passing through the recuperator, the remaining heat will provide hot water in a second heat exchanger (4). A brief summary of the mGT specifications is given in Table 1.

The current paper summarizes several series of simulations performed on the mGT cycle. A two-step procedure, developed by Bram and De Ruyck for the design of humidified gas turbine cycles has been used [21, 22]. This procedure has demonstrated its potential through the design of a new type of humid air cycle without saturation tower, the REgenerative EVAPoration cycle (REVAP®) [23, 24].

In this procedure, in a first step, the cycle layout is optimized by considering a general black-box heat recovery network where the exergy destruction is limited. In a second step, the corresponding heat recovery system is designed, using composite curve theory.

Through water injection in the mGT, some additional problems may rise. Two possible issues are the combustion stability and the reduction of the surge margin. The discussion of these issues falls outside the scope of this paper, however previous T100 mGT steam injection experiments resulted in stable operation of the engine [13].

3 Simulations of the water injection

The simulations presented in this paper, were performed with the Aspen® process simulator (version 2006.5), using previously developed models of the Turbec T100 mGT [8, 13].

3.1 Black box analysis

For the simulations performed in the first step of the 2-step method, all heat exchangers in the existing microturbine layout (the recuperator and the water heater) were replaced by a black

box heat recovery network. In the Aspen® process simulator a straightforward implementation of a black box is not possible, because no such component exists. In their paper, Bram and De Ruyck proposed a simple temporary network of heaters and coolers, that, as a whole, behaves like a black box with the proper boundary conditions [21]. Since the compressor of the T100 mGT consists of a single compressor stage and is very small, intercooling is not an option. Temperatures at the turbine inlet are also kept low (maximal 950°C) to avoid turbine cooling. The final scheme of the black box, used for the black box simulations of the T100 mGT in the Aspen® plus simulation tool, is given in Fig. 2.

The black box consists of one heater (HEATER) and one cooler (COOLER). All the water is injected in the outlet air of the compressor, resulting in a mixed vapour-liquid stream. After injection of water, the mixed stream is heated to saturation and further heated up to the imposed hot side pinch temperature (ΔT). The energy balance over the black box is expressed as indicated in Eq. (1).

$$\dot{Q}_{COOLER} + \dot{Q}_{HEATER} = 0 \tag{1}$$

By setting the stack temperature and the pinch on the hot side of the black box, the injected mass flow rate of water is fully determined, since there are only two degrees of freedom in the black box system. With these boundaries set, the only remaining variables in the black box system are the heat flux between the heater (HEATER) and the cooler (COOLER) and the injected mass flow rate. The other variables: $\dot{m}_{air}$, π and the produced power are changed and controlled by the mGT control system in order to reach the requested power at maximum TIT with a choked turbine.

3.1.1 Exergy analysis

The exergy destruction in the black box as a fraction of the exergy input in the global cycle is expressed in Eq. (2).

$$BB^{dest} = \frac{\sum_{in} \dot{E}x - \sum_{OUT} \dot{E}x}{\dot{E}x_{fuel}} \quad (2)$$

The exergy efficiency of the black box (Eq. (3)) is the ratio between the gain in exergy of the streams that are heated, and the loss in exergy of the streams that are cooled.

$$BB^{eff} = \frac{\sum_{gain} \Delta\dot{E}x}{\sum_{loss} \Delta\dot{E}x} \quad (3)$$

In this case Eq. (3) is reduced to the ratio between the exergy gain of the compressed air over the exergy loss of the exhaust gases.

As mentioned in [21], Aspen® does not have a build-in exergy function and an in-house Fortran procedure has been used for these simulations to calculated the exergy of the different streams.

3.1.2 Black box simulations

For the simulations, different stack temperatures and hot pinches are imposed. The exergy destruction over the black box is calculated (Eq. (2)) together with the exergy efficiency (Eq. (3)). In literature, values of exergy destruction of minimal 5% and a black box exergy efficiency as high as 93% are used as limits for the heat transfer systems [25]. Crossing these limits will lead to unrealistic designs, too difficult to realize with real heat exchangers. Boundary conditions used for the simulations are summarized in Table 2.

3.2 Grey box

The grey box design is the intermediate step between the black box and the final design developed using composite curves. The grey box consists of 3 heaters (SAT, HEATER1 and HEATER2) and 2 coolers (COOLER1 and COOLER2) (see Fig. 3). After water injection, the vapour-liquid mixture is saturated by adding heat in the SAT heater. After saturation, the air-

vapour mixture is heated further, using the HEATER1 and HEATER2 heaters, till the hot pinch temperature is reached. The exhaust gases are cooled till the applied stack temperature. Expressing the energy balance leads to Eq. (4).

$$\dot{Q}_{HEATER1} + \dot{Q}_{HEATER2} + \dot{Q}_{SAT} + \dot{Q}_{COOLER1} + \dot{Q}_{COOLER2} = 0 \tag{4}$$

Since the grey box is the intermediate step between the black box scenario and the real case, two extra conditions (Eq. (5) and (6)) are added to the heaters and coolers. The grouping of the different heaters and coolers occurs because in the final layout, it is the goal to work with two different heat exchangers, as is currently the case in the T100 mGT.

$$\dot{Q}_{SAT} + \dot{Q}_{HEATER1} + \dot{Q}_{COOLER2} = 0 \tag{5}$$

$$\dot{Q}_{COOLER1} + \dot{Q}_{HEATER2} = 0 \tag{6}$$

In order to meet this energy balance in combination with the boundary conditions previously set, the injected amount of water is adapted, since no extra degrees of freedom are added to the system compared to the black box approach.

Expressing the exergy destruction and efficiency over the grey box can be done in the same way as for the black box analysis. Results of the exergy analysis should be the same, since no major changes are made to the system. The different heaters and coolers of the black box systems have been split up, in order to come closer to the final layout, consisting of two heat exchangers.

3.3 Heat exchanger network design

In the second and final step of the two-step approach, the internal layout of the black box is determined, using composite curve theory. From these composite curves, the total cost of the heat exchangers can be estimated.

Rather than redesigning the whole heat exchanger network inside the T100, it was decided to keep the existing gas/gas recuperator and hot water heat exchanger and use these components for water injection. This leads to the design as depicted in Fig. 4.

A large amount of water is heated in the hot water heat exchanger. After the water is heated, it is injected in a saturation tower together with the compressor exhaust air in order to saturate this compressed air. Part of the water will evaporate till the compressor air is saturated. The saturated air is heated further by the hot exhaust gases of the turbine in the recuperator until the hot pinch temperature is reached, while the remaining water from the saturation tower is rerouted back to the heat exchanger, where extra feed water is injected in order to keep the total mass flow rate of water going through this heat exchanger and the saturation tower constant.

The main advantage of using this type of water introduction in the mGT cycle is that the original CHP installation remains unaffected. This allows the use of the mGT in CHP-mode during periods with heat demand and in water injection mode when there is no demand for heat. Eventually, it should be possible to use both modes at the same time, resulting in an mGT that produces continuously the nominal electrical power, independent of heat demand.

Another advantage of using a saturation tower instead of direct injection of water is the water quality. By letting a huge amount of water circulate through the system, only a small part of the circulated water will evaporate. When water injection occurs direct, all water will evaporate, so all contaminants present in the water will enter the mGT and foul the recuperator and turbine. With the evaporation tower, only a small part of the water evaporates, the contaminants remain in the water, so a lower feed water quality is demanded, resulting in a lower operational cost. For this reason, it was decided to use a saturation tower in combination with a water heater. If the design, proposed in the grey box layout would be

used, the remaining liquid water in the air entering the SAT heater (see Fig. 3) will completely evaporate, leaving behind al contaminants, resulting in heat exchanger fouling.

When the boundary condition are kept constant (design calculations), the total exergy destruction inside the heat exchanger network and the exergy efficiency of the system should stay the same, this for both the black and grey box, and be independent of the amount of circulating hot water; the circulating water does not leave the control volume and no additional exergy is added, the water only transports the energy.

With fixed heat exchange areas for the recuperator and hot water heater (off-design calculations), the exergy efficiency will change because of the changing boundary conditions. The question is whether the amount of circulating water will have an influence on the global exergy efficiency and exergy destruction. One should also take into account the control system of the microturbine itself. The maximal TIT of the T100 mGT is around 950°C; however the controller will set this temperature by keeping the Turbine Outlet Temperature (TOT) constant (645°C). Once water is added to the cycle, the thermodynamic properties of the gas/vapour mixture in the turbine will change. The controller however uses fixed correlation to estimate TIT out of the measurements of TOT. Once water is injected, the controller will underestimate TIT, resulting in a remarkable electric efficiency loss. For the final simulation, instead of controlling TIT, TOT is kept constant in order to be able to simulate the injection of water in the T100 microturbine as precisely as possible.

By letting water recirculate inside the heat exchanger network, an extra degree of freedom is added to the system. For the simulations, either the boundary conditions of the black box are applied to the heat exchanger network or the existing specifications of the heat exchangers are used. Even though an extra degree of freedom is added to the system, it is still not possible to set the injected amount of water. This amount of injected water is controlled by the saturation of the hot compressor exhaust air, while the amount of recirculation water can be chosen. This

corresponds to reality, where only the power of the pump, recirculating the hot water (not included in Fig. 4) can be controlled. In reality, an expansion vessel will be added to the system. Depending on the amount of water that evaporates in the saturation tower, the level inside this vessel will vary and a controller will add more or less water to the vessel in order to maintain the same level.

4 Results

All simulations performed for black box, grey box and white box approach were performed at nominal power of the T100 mGT, 100 kW. During simulations, isentropic turbine and compressor efficiency are kept constant, even though the mass flow rate through the compressor and working fluid properties of the turbine change as a consequence of the addition of water. On Fig. 5, the compressor map – used in the Aspen® plus simulations – with dry and wet operating line is shown. On the compressor map, it is clearly to see that the isentropic efficiency does not change between dry and wet operating point. For the turbine efficiency, previous research has shown that for an injection of 10 mass% of water, the efficiency only varies little (less than 0.1%) [16]. Next to the efficiencies, also the outlet pressure of the turbine and the pressure losses were kept constant. Even though the volumetric flow through heat exchangers and turbine will change due to water introduction and changing inlet air mass flow rate, the pressure loss in the hot/cold side of the heat exchanger is set as a design specification. Final heat exchanger design needs to be adapted in order to meet this design specification.

4.1 Black box

The results of the black box simulations are summarized in Fig. 6 till Fig. 12.

4.1.1 Water fraction

Fig. 6 shows the injected water fraction[1] versus the applied pinch on the hot side of the black box for different stack temperatures. As expected, a higher stack temperature leads to a reduced water fraction at constant pinch temperature on the hot side, since less energy is extracted from the exhaust gases for evaporating the water. The bigger the temperature difference between the inlet of the combustion chamber and the outlet of the turbine at constant stack temperature, the more the injected water fraction will increase. This can be explained as follows: at constant stack temperature, and taking into account that TIT remains constant, $\dot{Q}_{HOT}$ does not vary much, because the injected water fraction is rather low (maximal 5%), so the changes in heat capacity of the exhaust air are limited. So the same amount of heat needs to be absorbed in the heater (HEATER). In order to meet the boundary condition of a certain hot pinch, more water needs to be injected and evaporated with increasing pinch, since a lower combustor inlet temperature is required. The highest water fraction is obtained at the lowest stack temperature and highest pinch temperature.

4.1.2 Compressor performance

The T100 mGT operates always at constant power. The power output of the T100 mGT is controlled by changing the shaft speed. Once water is added to the cycle, the mass flow rate through the turbine will increase, while compressor mass flow rate remains constant, resulting in a higher turbine power and produced power. At this point, the controller of the T100 will interfere and reduce the rotation speed, in order to restore the generated power back to the requested power. The more water will be added, the more the rotation speed, and coupled the pressure ratio and inlet air mass flow rate will reduce. Fig. 7 gives the results of the changing

[1] The injected water fraction is defined as follows $\frac{\dot{m}_{water}}{\dot{m}_{total}}$ with $\dot{m}_{total} = \dot{m}_{water} + \dot{m}_{air}$

rotation speed, pressure ratio and compressor inlet air mass flow rate. The results are reduced, using the dry operation parameter. At nominal power (100 kW), the mGT runs at 66,700 rpm, resulting in a mass flow rate $\dot{m}_{air}$ of 0.70 kg/s and a pressure ratio π of 4.1.

4.1.3 Exergy analysis

Fig. 8 and Fig. 9 show the results of the exergy analysis. Black box exergy destruction is calculated using Eq. (2), while the exergy efficiency of the black box is calculated using Eq. (3).

Exergy efficiency

From Fig. 8 can be seen that the exergy efficiency of the black box decreases with increasing hot pinch, as expected. The higher the pinch temperature on the hot side of the heat exchanger network, the lower the outgoing exergy flow of the cold stream. The lower temperature is partially compensated by the higher water content of the air-vapour mixture but, as mentioned before, the maximum water fraction in the exhaust air is limited, and is not high enough to compensate for the lower outlet temperature of the cold stream. The influence of the stack temperature on the exergy efficiency is not as straight forward as that of the pinch temperature. For changing stack temperatures, the exergy efficiency only varies little (differences are smaller than 0.2%). At high pinch temperatures, exergy efficiency is slightly higher for lower stack temperatures. At lower pinch temperatures, exergy efficiency at higher stack temperatures becomes slightly bigger than at lower stack temperatures. The complex behaviour of the exergy efficiency as function of the stack temperature is a result of the different parameters influencing the in- and outgoing streams of the black box, e.g. the changing water fraction. The black box system is part of a bigger system, the mGT, where the controller tries to keep the produced electrical power constant, by changing the fuel flow and

the shaft speed, resulting in a different compressor mass flow, temperature and pressure. One can conclude that exergy efficiency is little affected by stack temperature.

Network exergy destruction

When looking at the exergy destruction, which must be positive as required by the second law expressed over the black box, one can deduct from Fig. 9 that exergy destruction will increase with increasing hot pinch and decreasing stack temperature. The increasing exergy destruction with increasing hot pinch temperature corresponds well with the calculated exergy efficiencies from Fig. 8. The higher the pinch temperature, the more exergy will be destructed in the heat exchanger, resulting in a lower efficiency. The stack temperature seems to have a bigger influence on exergy destruction. With increasing stack temperature, the exergy destruction will also decrease. The complex influence of the other parameters seems to have disappeared by taking the difference between the in- and outgoing exergy flows (see Eq. (2), resulting in a straight forward correlation between stack temperature and exergy destruction. Even though exergy efficiency varies little at constant hot pinch, exergy destruction changes due to the changing properties of the gases because of the changing water fraction.

On Fig. 9 one can see that there is a remarkable difference between the decreasing exergy destruction from 80°C to 90°C and from 110°C to 120°C. This difference results from altered composition, resulting in a non-linear decreasing exergy destruction.

Both Fig. 8 and Fig. 9 show that black box exergy efficiency and exergy destruction are below the limits that can be found in literature [25] so all scenarios should be feasible. For gas/gas heat exchanger having acceptable pressure losses and a hot pinch of 50°C is consider as economically viable. Stack temperatures lower than 90°C should be avoided, in order to avoid condensation of the water in the heat exchanger. The lower exergy efficiency is completely in line with conclusions of Zhang et al. [20].

Component exergy destruction

In order to gain an insight in which components are crucial in the black box, an analysis of the exergy destruction in the different components is made. Fig. 10 shows that for a small pinch, the destruction in the heat exchanger (heater (HEATER) and cooler (COOLER) combined together) is nearly twice as big as the destruction in the mixer. With increasing pinch temperature, the exergy destruction in the heat exchanger increases dramatically. On the other hand, the exergy destruction by mixing the water with the compressed air decreases with increasing hot pinch. The decreasing mixing exergy loss can be explained as follows: as indicated on Fig. 6, the injected fraction of water increases with increasing hot pinch. Since the T100 microturbine always operates at constant produced electric power, the compressor will slow down, resulting in a decreasing air mass flow, pressure ratio and especially a lower air temperature. Through the decreasing compressed air inlet temperature, water and air temperature match better for mixing, resulting in a lower exergy destruction. The stack temperature has no influence on the mixing exergy loss, even though more water is injected at lower stack temperature. The mixing exergy loss remains constant through the increasing exergy input in the cycle because of the higher fuel flow, which results in a lower efficiency (see Fig. 11). By matching injection temperatures better, the exergy destruction in the final layout of the microturbine heat exchanger network can be reduced in order to obtain a better performance.

4.1.4 Composite curves

Fig. 12 gives the composite curves of the black box system, calculated using a temperature difference at the hot side of the heat exchanger system of 50°C, which is an acceptable value for a gas/gas heat exchanger and a final stack temperature of 90°C, in order to avoid problems with condensation of water inside the heat exchanger. These boundary conditions will be used

for further design of the heat exchanger network. The mixing of the air and water is introduced into the composite curves as a heat exchanger, where the cold stream corresponds to the injected water and the hot stream to the compressed air. The minimal pinch in Fig. 12 is 27°C.

4.1.5 Electric efficiency

Fig. 11 gives the results of the absolute electric efficiency rise of the T100 mGT when injecting water. As can be expected, the electric efficiency will increase with decreasing stack temperature and hot pinch temperature, since more energy is recuperated with a lower stack temperature and less fuel is required to reach the maximal TIT with a smaller temperature difference on the hot side. The corresponding dry case efficiency (with TIT equal to 950°C) results in an electric efficiency of 32.7%, showing that with a hot pinch of 50°C and a stack temperature of 90°C, the efficiency could be increased by 7% compared to the dry-case mGT. Since the produced electrical power of the T100 remains constant, the injection of the water will lead to a reduction in fuel consumption. With 6% of the total mass flow rate replaced by water, the total fuel consumption can be decreased with 18%. Compared to the injected water fraction, depicted in Fig. 6, the resulting absolute electric efficiency increase seems to be a little bit contradictory. One should expect that the total electric efficiency will increase with increasing water fraction; however results from simulations show the opposite. The previous statement is only true when all other parameters are kept constant. In these simulations, the water mass flow rate is used to reach several boundary conditions and so the injected water mass flow is determined by the boundary conditions. So the boundary conditions (hot pinch and stack temperature) determine the electric efficiency of the mGT.

4.2 Grey box

4.2.1 Exergy analysis

Fig. 13 and 14 give the comparison of the exergy efficiency and exergy destruction of the black box and the grey box at different hot pinch temperatures and stack temperatures. As expected, when the same boundary conditions are applied to the system, both exergy efficiency and destruction are the same for the black and grey box system.

An analysis of the destruction of exergy, shown in Fig. 15 in the different components, shows that the exergy destruction in the mixing process decreases with increasing pinch, while the exergy destruction in both heat exchangers[2] increases with increasing pinch. The same explanation as for the black box can be used to explain the results from the grey box exergy analysis, shown in Fig. 15.

4.2.2 Composite curves

The composite curves (see Fig. 16) are now slightly different than the ones of the black box simulations (Fig. 12), due to the split of the heat exchangers. The hot curve remains the same, because the composition of the exhaust gas going through coolers COOLER1 and COOLER2 neither the temperature of the compressor exhaust air did change. The cold curve changes, due to the split up of the heaters into a saturator (SAT) and two heaters (HEATER1 and 2). The minimal pinch in Fig. 16 has slightly increased to 50°C.

4.3 White box case

The final part of the simulations is the one conducted on the existing layout of the microturbine.

[2] The Exchanger1 corresponds to heaters SAT and HEATER1 and cooler COOLER2 from the grey box layout, while the Exchanger2 corresponds to heater HEATER2 and cooler COOLER1.

4.3.1 Exergy analysis

Fig. 17 shows the effect of the recirculated mass flow on the total exergy destruction and efficiency in the heat exchange network using varying boundary conditions. As expected, the applied mass flow rate has no effect on exergy destruction and efficiency, when the boundary conditions are kept constant. For all simulations performed in this part of the study, a hot pinch temperature of 50°C has been used in combination with a stack temperature of 90°C. Fig. 17 also shows that the exergy destruction and efficiency are the same as for the black box with the same boundary conditions, as was expected.

Fig. 17 clearly showed that the destruction of exergy is independent of the circulating water flow, when applying the same boundary conditions as for the black box. The question is: does the mass flow rate of circulating water have an influence when taking into account the limitations of the installed heat exchangers in the T100 mGT (the limited surface for heat exchange) and the control system of the mGT (keeping TOT constant instead of TIT)?

Fig. 17 illustrates that with fixed heat exchange areas for the recuperator and hot water heater (off-design calculations), the exergy efficiency will decrease. The use of existing heat exchangers results in a higher stack temperature (which has little effect on exergy efficiency) and a higher hot pinch temperature (which has a severe negative effect on the exergy efficiency; see results black box simulations). As also can be deducted from the results of simulations, using the existing heat exchangers or new ones (see Fig. 17), it is clear that the circulating water flow rate has no effect on the global exergy destruction and efficiency of the heat exchangers network. The recirculation flow rate has however a huge effect on the temperature of the injected water and a minor effect on the final stack temperature (see Fig. 18). The higher stack temperature will lead to a higher exergy loss through the stack, what should result in lower exergy efficiency, however the water fraction in the exhaust gases is very low and this in combination with a very small increase, leads to an insignificant

difference, as shown in Fig. 17. When looking at the exergy destruction in the different components of the network (Fig. 19), it is easy to see that the destruction inside the recuperator remains constant, since the same amount of water is evaporated in the compressed air. The exergy destruction in the water heater is lower at lower water mass flows, because the outlet water temperature is higher, as can be seen on Fig. 18. The mixing exergy destruction is higher at lower mass flow rates, even though the water temperature is higher and better matches the air temperature. However in this case, both water and air will cool down, due to evaporation, so the mixing temperature is lower than water temperature (79°C), so at lower flow rates, the temperature difference between in and outlet will be higher, resulting in a higher exergy destruction. Both phenomenon's counteract, resulting in a network exergy destruction independent of the water flow rate. The recirculating mass flow rate has a huge impact on the size of the saturation tower. The mass flow rate will determine the total volume of the saturation tower required to saturate the compressed air. One should also take into account the pump power, necessary to increase the water pressure to compensate the head losses in the water circuit. The higher the water flow, the more produced electrical power by the mGT is needed for the auxiliaries, the lower the electric efficiency will be. Fig. 20 shows the impact of the power pump, necessary to compensate the head losses (0 bar case), on the total efficiency of the mGT. Losses are expressed as absolute efficiency losses. The necessary pump power is rather low (maximal 0.11 kW at a circulating water mass flow rate of 5 kg/s), which results in a minimal effect on global efficiency (absolute loss in efficiency of 0.04% at 5 kg/s mass flow rate). Commonly, the water is introduced in the saturation tower by means of injection nozzles. For these nozzles, a certain pressure difference is necessary to obtain a minimal mean droplet diameter. In Fig. 20, results of the effect of increasing the injection pressure of the water (0 bar to 5 bar pressure difference) in the saturation tower on global mGT efficiency are shown. Results show that increasing the injection pressure (up to 5 bar)

and circulating mass flow rate (maximal 5 kg/s) has a huge effect on cycle efficiency (absolute loss in efficiency of 1.5%). For the final design of the saturation tower, a trade-off between size and pumping power needs to be found. Due to the limitations of the heat exchangers, the temperature difference between the inlet of the combustion chamber and the TOT will increase with an increasing stack temperature, resulting in higher exergy destruction and efficiency (Fig. 21). This has a severe negative effect on the total electric efficiency of the microturbine cycle, as can be seen on Fig. 22. On Fig. 21 and 22, simulations results of designing a new heat exchanger network (Case New) are compared with results using the existing heat exchangers in the network (Case Exist).

When taking into account the modus operandi of the control system – meaning keeping TOT constant (Case TOT) instead of TIT (Case TIT) – exergetic efficiency will drop even more.

4.3.2 Electric efficiency

Due to the decreasing exergetic efficiency and increasing exergy destruction, the total efficiency of the microturbine cycle will be affected, as can be seen in Fig. 22. Since Fig. 17 showed that the results are independent of the recirculating water flow rate, Fig. 21 and Fig. 22 only show the results of simulations performed using 2.5 kg/s circulating water, since the water flow rate has no effect on global energy and exergy efficiency. The difference between the exergy efficiency and destruction at constant TIT or TOT are limited, however the energetic efficiency is more influenced by keeping TOT constant instead of TIT, because a constant TOT results in a lower TIT and higher exergy destruction in the combustion chamber, which results in a lower global electric efficiency.

The final simulation results from Fig. 22 show an absolute increase of 2% in electric efficiency, when water injection is applied. As simulations showed clearly, a higher electric efficiency can be reached by adapting the control system of the mGT. For the T100, once the

power output is set, the existing control system will fulfil this demand by controlling the shaft speed and controlling the fuel flow. As mentioned before, fuel flow is controlled to keep TIT below a certain limit (950°C), which is dangerous for the turbine inlet. Measuring TIT is not possible due to technical limitations; instead TOT is measured and controlled. By using fixed lookup tables, as mentioned before, TIT is estimated out of this TOT measurement. When injection of steam occurs, these lookup tables however are no longer valid, since the heat capacity of the medium has increased, due to the addition of water. Using the measured TOT in combination with the lookup tables in this case will result in a TIT that is underestimated, meaning there is still margin to increase TOT without damaging the turbine inlet. A lower TIT has a direct negative impact on turbine efficiency. For the Aspen® plus simulations, the same control principle has been used, meaning the natural gas flow rate is controlled by a TOT control system (keeping TOT constant at 645°C) and the rotation speed of the compressor is controlled by the output power control (keeping the generated power equal to the set power, 100kW for all simulations in this paper). Adapting the TOT controller to a TIT control mechanism in Aspen® plus is rather simple, since TIT values are directly available in simulations, however adapting the control system of the T100 would require an additional measurement of the water content in the flue gases. In order to reach optimal steam injection, the following adapted control mechanism for the T100 is proposed. An additional sensor to measure water content in the flue gases gives additional information to the control system about the composition of the flue gases. Based upon this composition, in combination with the measurement of TOT, using new lookup table, composition dependant, TIT can be estimated. This allows a more precise TIT control and allows to T100 to fully perform at its maximal possible TIT, independent of possible steam/water injection.

Fig. 22 also shows that with existing heat exchangers, more water will be evaporated, which corresponds to the results of the black box simulations: the lower the exergy efficiency, the higher the evaporative mass flow rate.

As a small case study, the influence of redesigning only one of the two existing heat exchangers has been examined. The results of the case study are added to Fig. 21 and 22 and show that redesigning the recuperator can increase the performance of the heat exchanger network significantly (Case New R), while changing the water heat exchanger only has a minor effect on global performance of the T100 (Case New WH). Even with only an adapted recuperator, a stack temperature of 88°C can be reached. The lower stack temperature explains the very high exergy efficiency and low exergy destruction (as low as the black box) from Fig. 21. The final energetic efficiency is however still lower than the black box efficiency (see Fig. 22), due to the higher exergy destruction in the combustion chamber when operation at constant TOT instead of constant TIT.

Final changes in rotation speed, compressor air mass flow rate, $\dot{m}_{air}$, and pressure ratio π are shown in Fig. 23**.**

4.3.3 Composite curves

The final composite curves of the existing system can be found in Fig. 24.

For the construction of the composite curves, the saturation tower has been excluded, since it is not possible to split the different streams into hot and cold streams. Both, water and air inlet stream cool down inside the saturation tower, because a small amount of the water will evaporate and extract sensible heat from both the water and air stream. The removal of the saturation tower from the composite curves results into a jump in the hot curve. At 12 kW, the pinch amounts only 1.1°C, which does not cause any problems, because it is the result of the mixing process between the hot water, coming back from the saturation tower and the cold

feed water. The injected mass flow rate of feed water is very low compared to the recirculating water flow rate, so equilibrium should be reach without problems. The minimal pinch for the heat exchange system is now 22.6°C, at water heater.

4.4 Technical remarks

During all simulations performed in this paper, generic heat exchangers – except for the cases where the existing heat exchangers were used – were implemented into Aspen® plus simulation engine. For each different case, with different mass flow rate, gas composition and maximal heat exchange, the heat exchangers needs to be redesigned, taking into account the fixed pressure losses, mentioned in Table 2, as design specifications. For the recuperator, typically a primary surface counter flow heat exchanger with cross corrugated duct configuration heat exchanger is used [9]. In order to meet the requirements of heat transfer and limited pressure losses, the total surface of the heat exchanger needs to be changed with changing maximal heat transfer. To limit pressure drop, the size of the different channels needs to be adapted, depending on the volume flows. Actual design of the new heat exchangers for the different case is however outside the scope of this paper. For the water heat exchanger, a typical cross flow shell-tube heat exchanger, as is currently installed in the T100 will be used [26].

During simulations of the heat exchanger network, using the existing heat exchangers, constant pressure drops were assumed, however due to water injection, flow specification will change. Due to the injection of water, the mass flow rate reduces. In combination with this mass flow rate reduction, volume flow and density will also change, resulting in lower pressure losses (29% on cold side of the recuperator, 10% on turbine exhaust). By keeping the pressure losses constant, the final performance and electrical efficiency of the mGT is underestimated by 0.4%. It was chosen not to adapt the pressure losses, since it is difficult to

predict pressure loss in the water saturation tower. By keeping the pressure loss constant, efficiency increase is determined in a conservative way.

Another important component of the final cycle layout is the saturation tower. The saturation tower needs to fully saturate the compressed air. No complete saturation of the air will consequently lead to a reduced performance of the mGT. Tree major design specifications for the saturation tower will be the pressure loss, size of the saturation tower and total investment cost. Pressure losses need to be minimized, since a 1% pressure loss decrease will increase mGT efficiency by about 0.33% [27]. Parente et al. simulated that the total humidifier tower packing for a 100 kW mGT would be 0.08 m^3 [16] and the additional investment cost for the tower would be 100 €/kW installed power [17].

5 Conclusion

The results of a series of simulations of water injection in the compressor outlet of an mGT are presented. Water injection can increase the number of running hours of an mGT by keeping it in operation in periods with lower heat demand. The injected water is preheated with heat from the mGT recuperator exhaust. Simulations show that water injection increases the electric efficiency of the mGT. To find the maximal potential for water injection in a T100 mGT, the heat recuperating and water injection systems are represented by a black box system. The boundary conditions are the stack temperature and the hot pinch. From these black box simulations, a new design for a heat exchange network is proposed. The design is based on the existing recuperator and hot water heater of the T100 unit. Water is brought into the engine by means of a saturation tower trough which a large amount of water is circulated.

Black box design calculations showed that when 6% of the total mass flow of air is replaced by water, 18% fuel can be saved and an absolute electric efficiency increase of 7% is obtained.

The final stack temperature and hot pinch, imposed as boundary conditions on the heat exchange network, have a direct influence on the exergy destruction and efficiency of the black box and also on the maximum water injection flow rate.

Black box off-design simulations showed that exergy destruction and efficiency of the heat exchanger network are only effected by the applied boundary conditions. On top of that, for a fixed set of boundary conditions, the efficiency of the network does not depend on the circulating water mass flow rate.

A final series of simulations, taking into account the properties of the control system of the T100 mGT and based on the existing heat exchangers installed in the T100, showed that the maximal achievable final exergy and energy efficiency is lower than the black box simulations indicated, with only 2% absolute increase in efficiency, when 2.5 kg/s of water is recirculated.

6 Future work

Experiments of steam injection have shown the potential of water/steam introduction in a T100 mGT. Simulations of the potential of the T100 for water injection showed the exergetic limit of water injection and helped developing a heat exchanger network, existing out of a water heater, a recuperator and an evaporation tower. The only new component in the cycle is the evaporation tower.

The next step of the research is focussed on this evaporation tower. Knowing its boundary conditions, one can start designing this tower. Requirements of the component will be: minimal pressure losses inside the tower, minimal injection pressure of the water and minimal size of the tower in order to keep the operational cost (power loss of the mGT and pump power needed for the water) and the investment cost as low as possible. It is clear that a trade-off between the different design criteria should be made.

Since the lower TIT has a very negative effect on the global efficiency of the mGT, changing the control system of the T100 should also be considered.

Acknowledgement

The research was funded by the National Fund for Scientific Research (FWO).

Reference

[1] Gamou S, Ito K, Yokoyama R. Optimal Operational Planning of Cogeneration Systems With Microturbine and Desiccant Air Conditioning Units. Journal of Engineering for Gas Turbines and Power. 2005;127:606-14.

[2] Gamou S, Yokoyama R, Ito K. Parametric Study on Economic Feasibility of Microturbine Cogeneration Systems by an Optimization Approach. Journal of Engineering for Gas Turbines and Power. 2005;127:389-96.

[3] Kalantar M, Mousavi G SM. Dynamic behavior of a stand-alone hybrid power generation system of wind turbine, microturbine, solar array and battery storage. Applied Energy. 2010;87:3051-64.

[4] Sanaye S, Ardali MR. Estimating the power and number of microturbines in small-scale combined heat and power systems. Applied Energy. 2009;86:895-903.

[5] Katsigiannis PA, Papadopoulos DP. A general technoeconomic and environmental procedure for assessment of small-scale cogeneration scheme installations: Application to a local industry operating in Thrace, Greece, using microturbines. Energy Conversion and Management. 2005;46:3150-74.

[6] Pilavachi PA. Mini- and micro-gas turbines for combined heat and power. Applied Thermal Engineering. 2002;22:2003 - 14.

[7] Kaikko J, Backman J. Technical and economic performance analysis for a microturbine in combined heat and power generation. Energy. 2007;32:378 - 87.

[8] Delattin F, Bram S, Knoops S, De Ruyck J. Effects of steam injection on microturbine efficiency and performance. Energy. 2008;33:241-7.

[9] Heppenstall T. Advanced gas turbine cycles for power generation: a critical review. Applied Thermal Engineering. 1998;18:837 - 46.

[10] McDonald CF. Low-cost compact primary surface recuperator concept for microturbines. Applied Thermal Engineering. 2000;20:471 - 97.

[11] McDonald CF. Recuperator considerations for future higher efficiency microturbines. Applied Thermal Engineering. 2003;23:1463-87.

[12] Massardo AF, McDonald CF, Korakianitis T. Microturbine/Fuel-Cell Coupling for High-Efficiency Electrical-Power Generation. Journal of Engineering for Gas Turbines and Power. 2002;124:110-6.

[13] De Paepe W, Delattin F, Bram S, De Ruyck J. Steam injection experiments in a microturbine – A thermodynamic performance analysis. Applied Energy. 2012;97:569-76.

[14] Jonsson M, Yan J. Humidified gas turbines—a review of proposed and implemented cycles. Energy. 2005;30:1013-78.

[15] Rao AD, Day WH. HAT cycle status report. Eleventh conference on gasification power plants. Sheraton Palace Hotel, San Francisco, California1992.

[16] Parente J, Traverso A, Massardo AF. Micro Humid Air Cycle: Part A --- Thermodynamic and Technical Aspects. ASME Conference Proceedings (ASME Paper GT2003-38326). 2003;2003:221-9.

[17] Parente J, Traverso A, Massardo AF. Micro Humid Air Cycle: Part B --- Thermoeconomic Analysis. ASME Conference Proceedings (ASME Paper GT2003-38328). 2003;2003:231-9.

[18] Lee JJ, Jeon MS, Kim TS. The influence of water and steam injection on the performance of a recuperated cycle microturbine for combined heat and power application. Applied Energy. 2010;87:1307 - 16.

[19] Dodo S, Nakano S, Inoue T, Ichinose M, Yagi M, Tsubouchi K, et al. Development of an Advanced Microturbine System Using Humid Air Turbine Cycle. ASME Conference Proceedings (ASME Paper GT2004-54337). 2004;2004:167-74.

[20] Zhang S, Xiao Y. Steady-State Off-Design Thermodynamic Performance Analysis of a Humid Air Turbine Based on a Micro Turbine. ASME Conference Proceedings (ASME Paper GT2006-90335). 2006;2006:287-96.

[21] Bram S, De Ruyck J. Exergy analysis tools for Aspen applied to evaporative cycle design. Energy Conversion and Management. 1997;38:1613-24.

[22] Bram S, De Ruyck J. Exergy analysis and design of mixed CO2/steam gas turbine cycles. Energy Conversion and Management. 1995;36:845-8.

[23] De Ruyck J, Bram S, Allard G. REVAP® Cycle: A New Evaporative Cycle Without Saturation Tower. Journal of Engineering for Gas Turbines and Power. 1997;119:893-7.

[24] De Ruyck J, Bram S, Allard G. Humid air cycle development based on exergy analysis and composite curve theory. ASME Conference Proceedings (ASME Paper 95-CTP-39). 1995;1995.

[25] El-Masri MA. A Modified, High-Efficiency, Recuperated Gas Turbine Cycle. Journal of Engineering for Gas Turbines and Power. 1988;110:233-42.

[26] Luvata. Industrial Heat Exchangers: QMXF - Steel coils. Retrieved from *http://www.luvata.com/en/Products--Markets/Products/Heat-Transfer-Solutions/Special-Industrial-Products1/Industrial-Heat-Exchangers/* October 2012.

[27] Lagerstrom G, Xie M. High Performance and Cost Effective Recuperator for Micro-Gas Turbines. ASME Conference Proceedings (ASME Paper GT2002-30402). 2002;2002:1003-7.

Figures

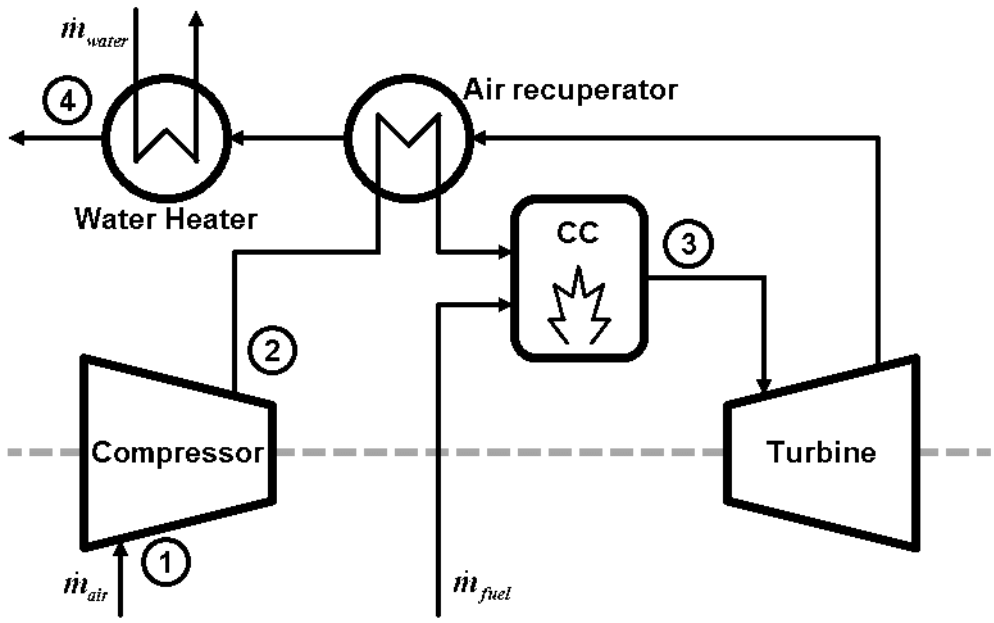

Figure 1: Microturbine layout.

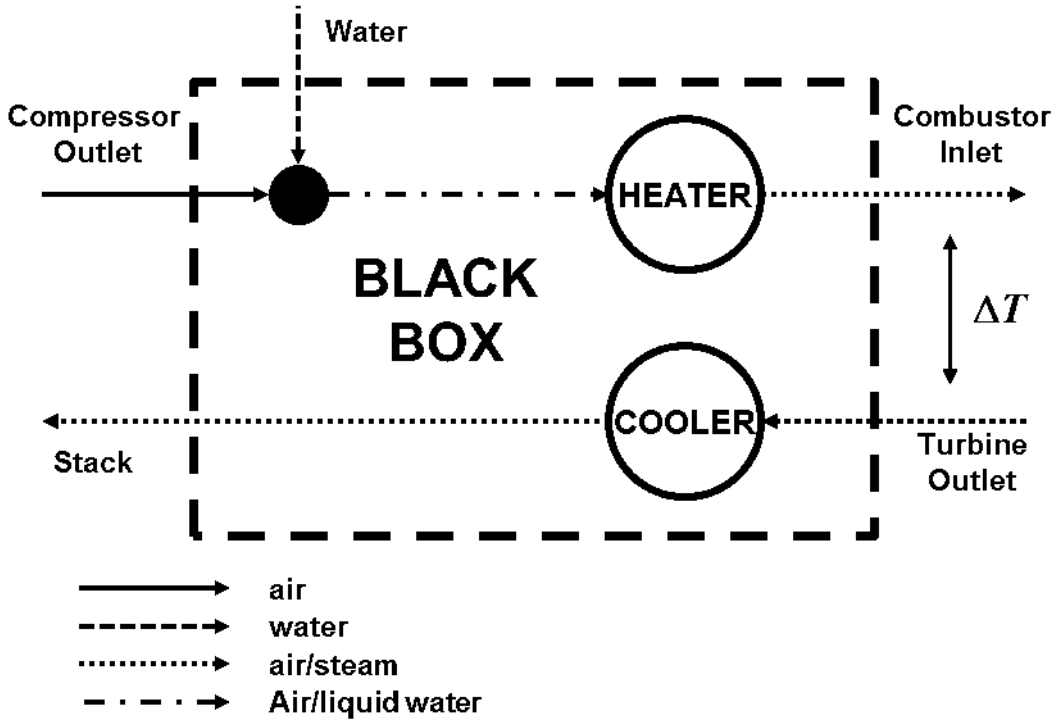

Figure 2: Black box with heater and cooler.

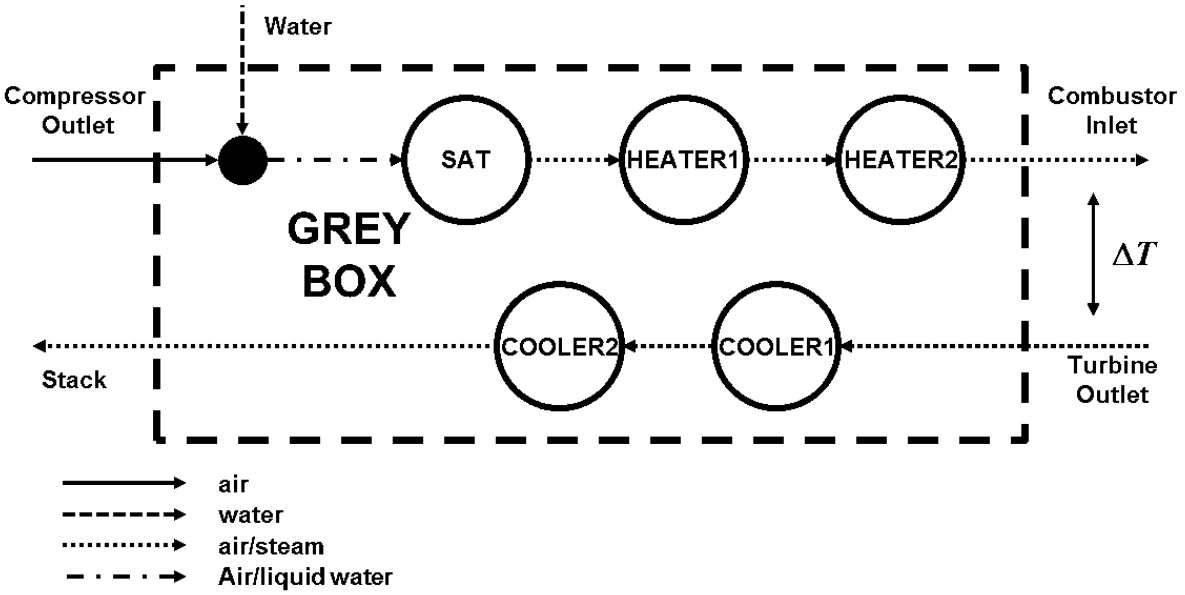

Figure 3: Grey box layout with heaters and coolers.

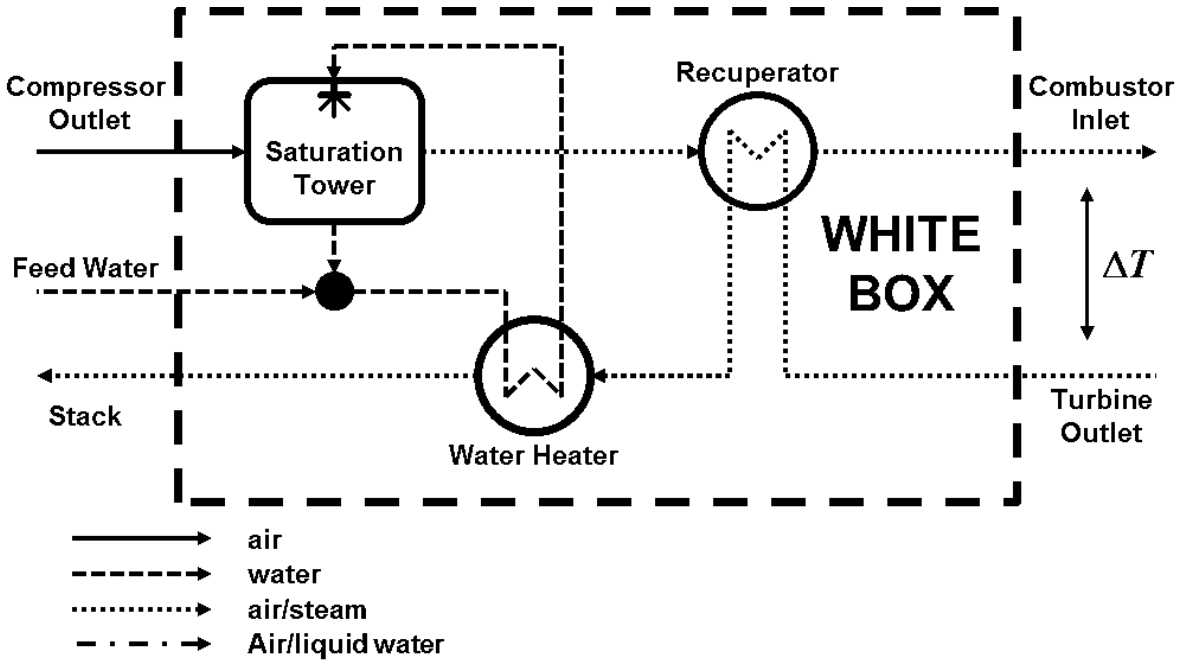

Figure 4: White box design of the heat exchanger network for the Turbec T100 mGT.

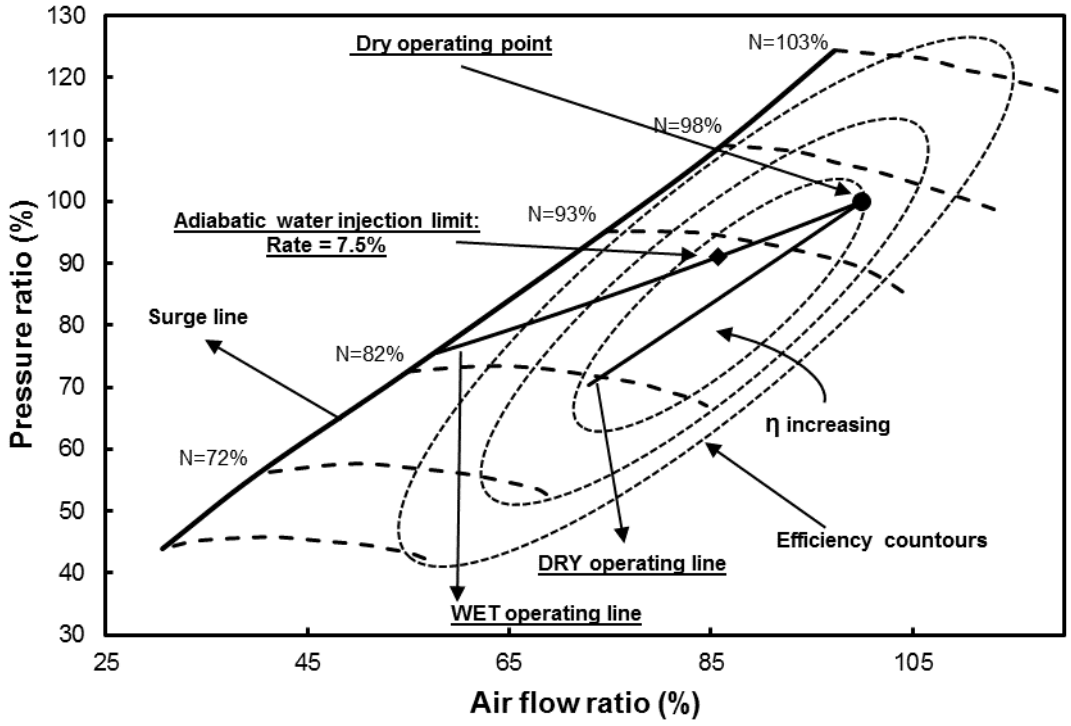

Figure 5: Compressor map with indicated dry and wet operating lines at nominal electrical power.

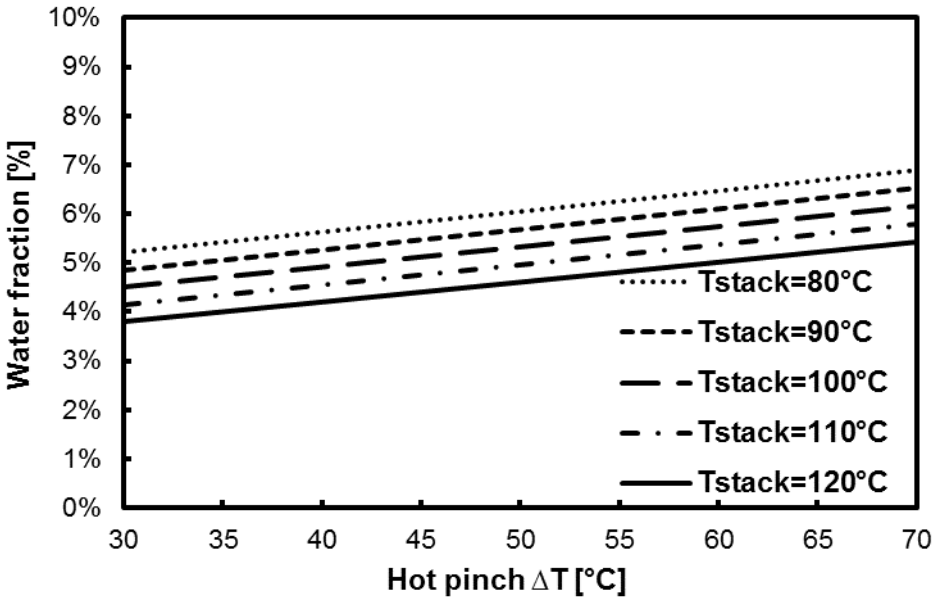

Figure 6: Water injection rate for the different scenarios.

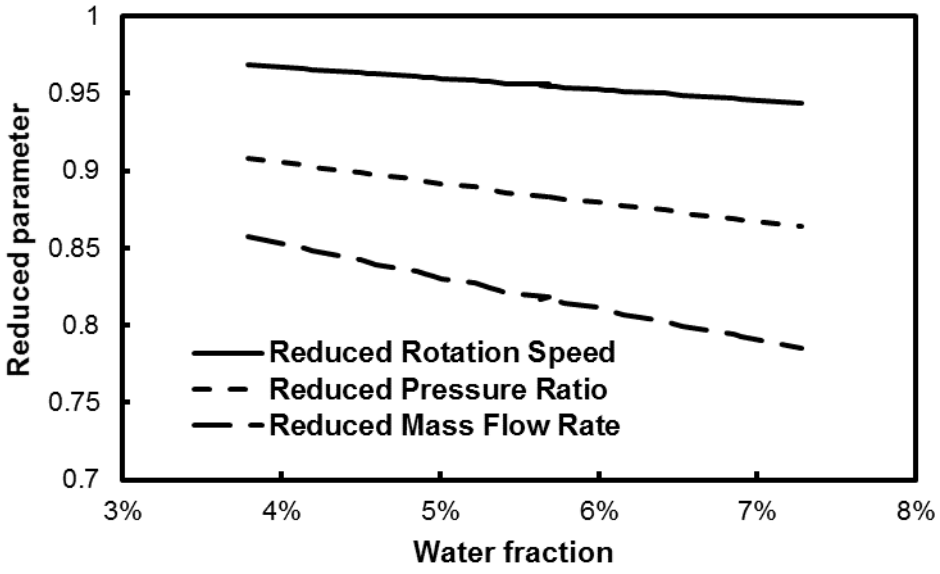

Figure 7:Reduced rotation speed, mass flow rate and pressure ratio for different scenarios.

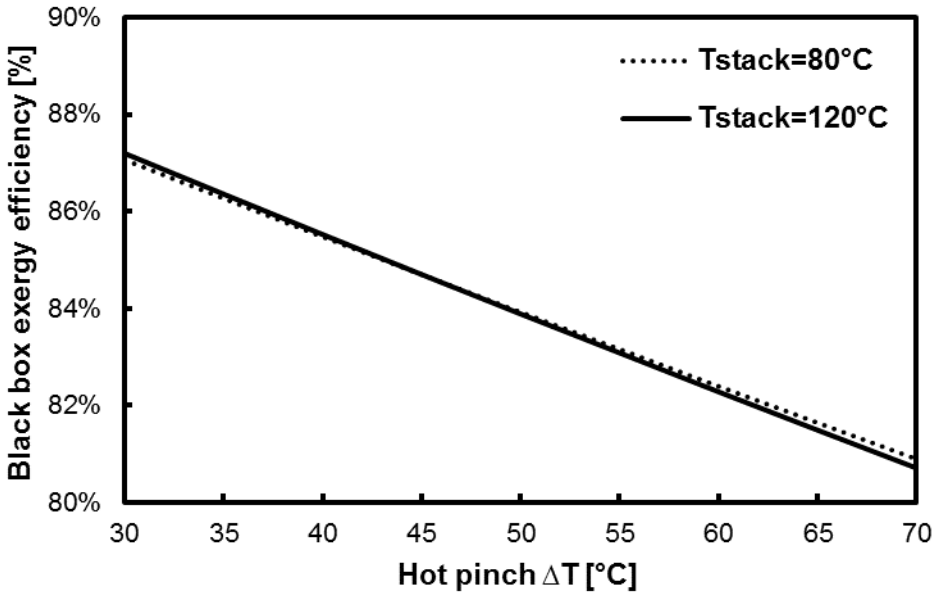

Figure 8:Exergy efficiency of the black box heat exchanger system for the different simulation scenarios.

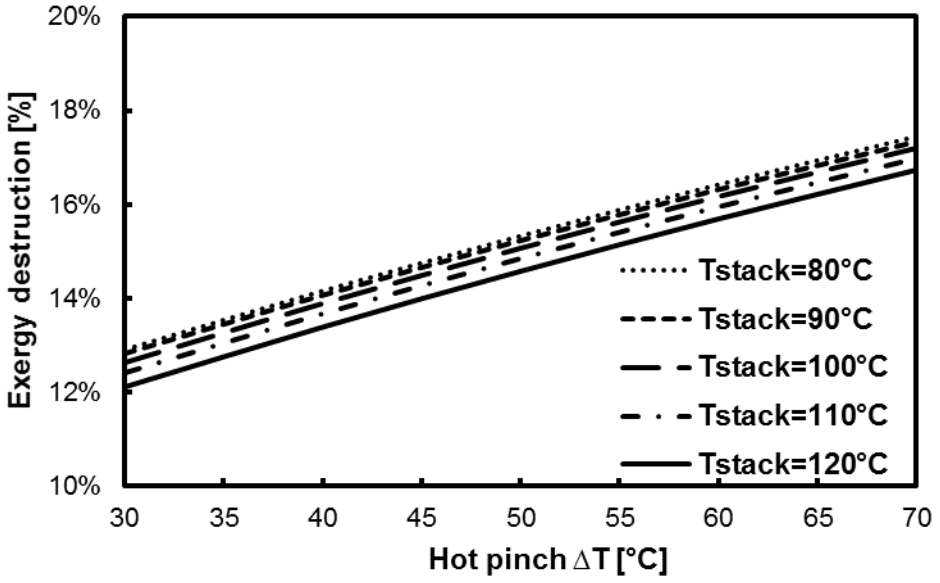

Figure 9:Exergy destruction in the black box for the different simulation scenarios.

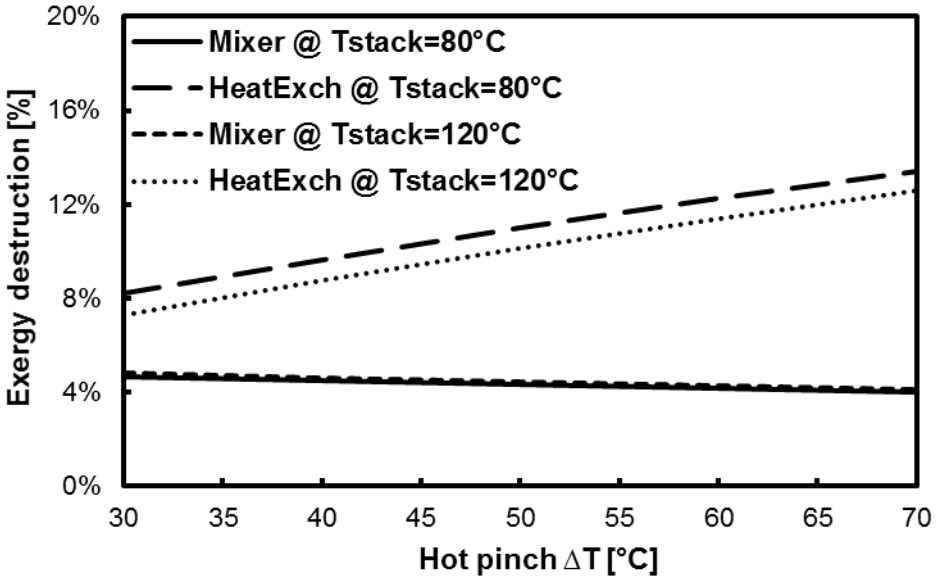

Figure 10: Exergy destruction by component of the black box system.

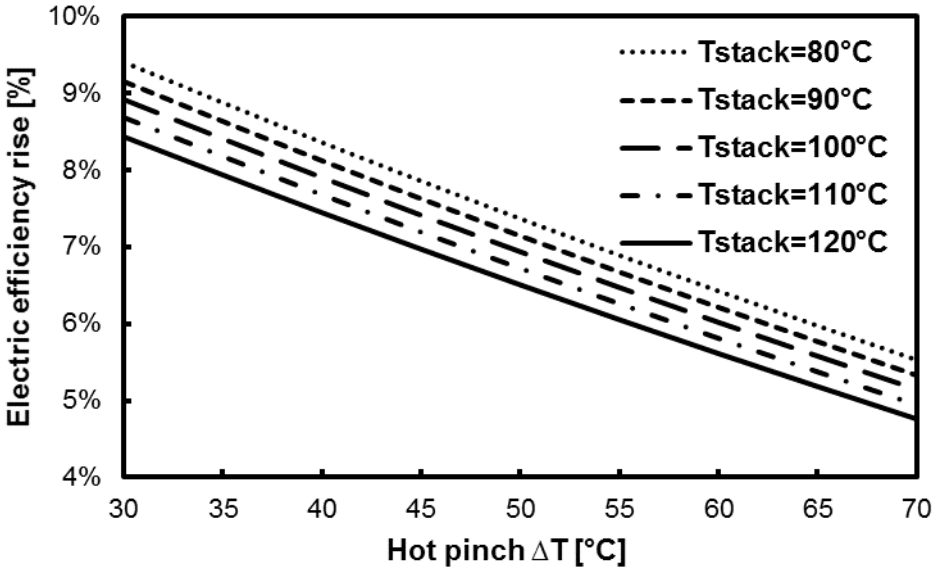

Figure 11: Electric efficiency of the mGT for different simulation scenarios.

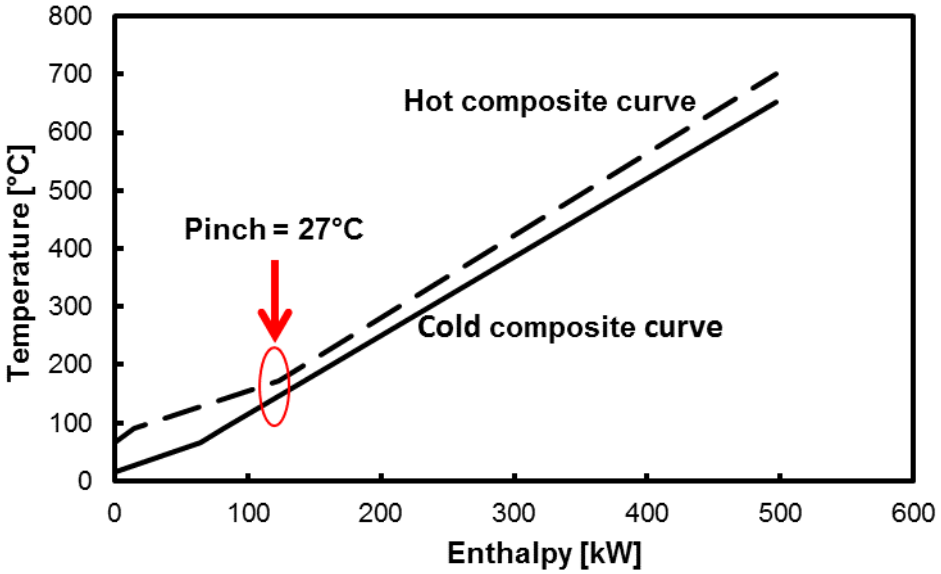

Figure 12:Composite curves of the black box heat exchangers system.

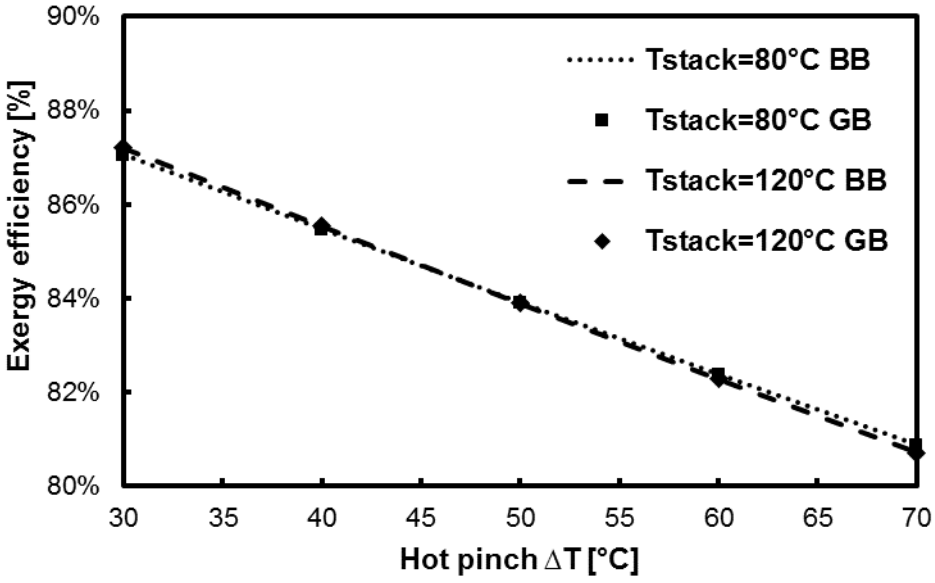

Figure 13:Comparison black box (BB) and grey box (GB) exergy efficiency.

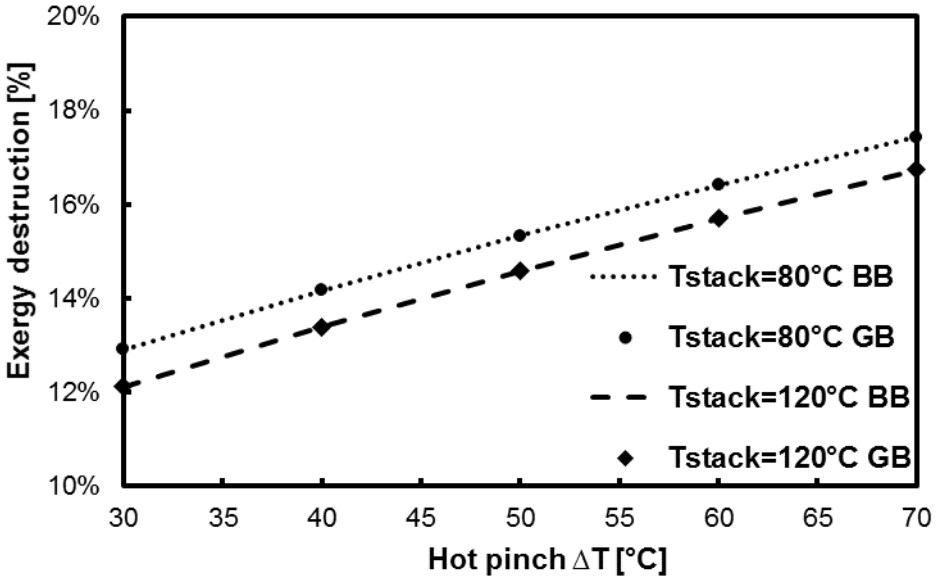

Figure 14: Comparison black box (BB) and grey box (GB) exergy destruction.

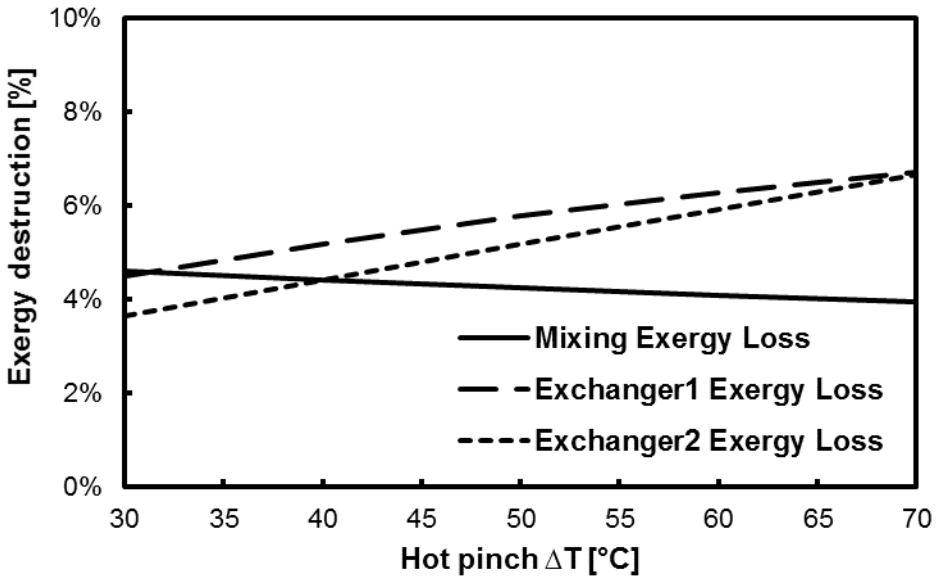

Figure 15: Exergy loss in the different components of the grey box using a fixed stack temperature of 90°C.

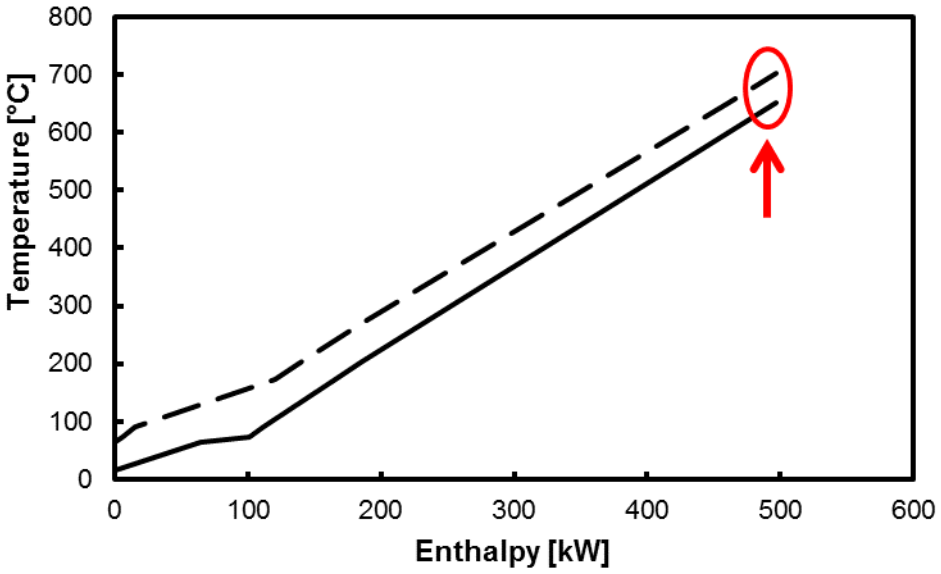

Figure 16: Composite curve of the grey box using a hot pinch of 50°C and a stack temperature of 90°C.

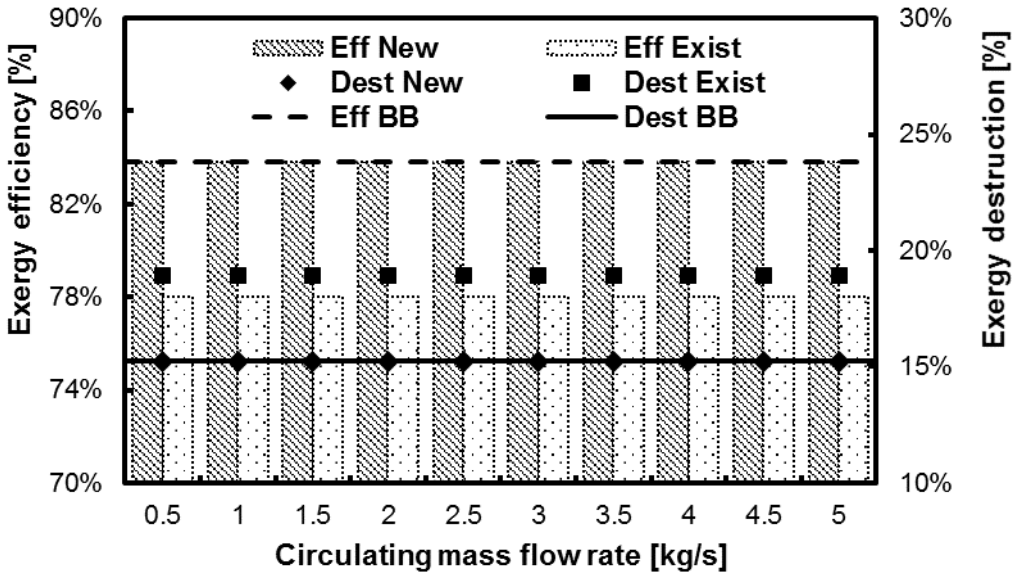

Figure 17: Exergy efficiency and destruction of the heat exchanger network, using new heat exchangers (New) and using the existing once (Exist), compared to the black box (BB) efficiency and destruction.

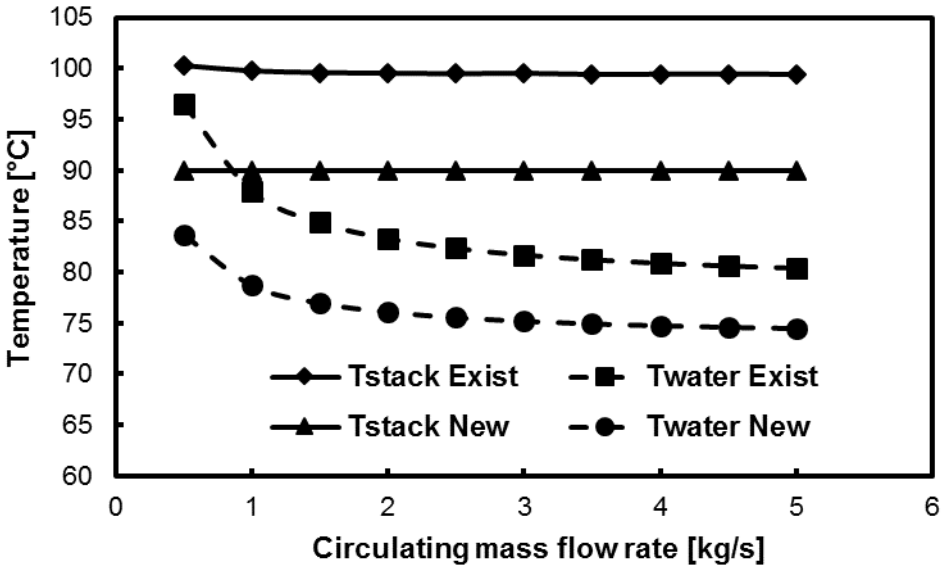

Figure 18: Stack (Tstack) and temperature of the injected water in the saturation tower (Twater) at different recirculation flow rates.

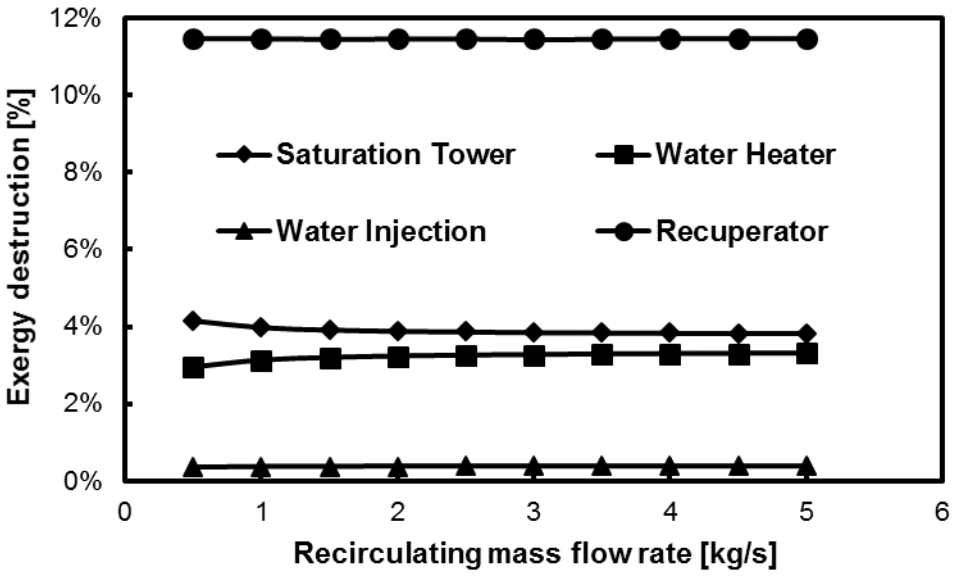

Figure 19: Exergy destruction in the different components of the existing heat exchanger network at constant TIT.

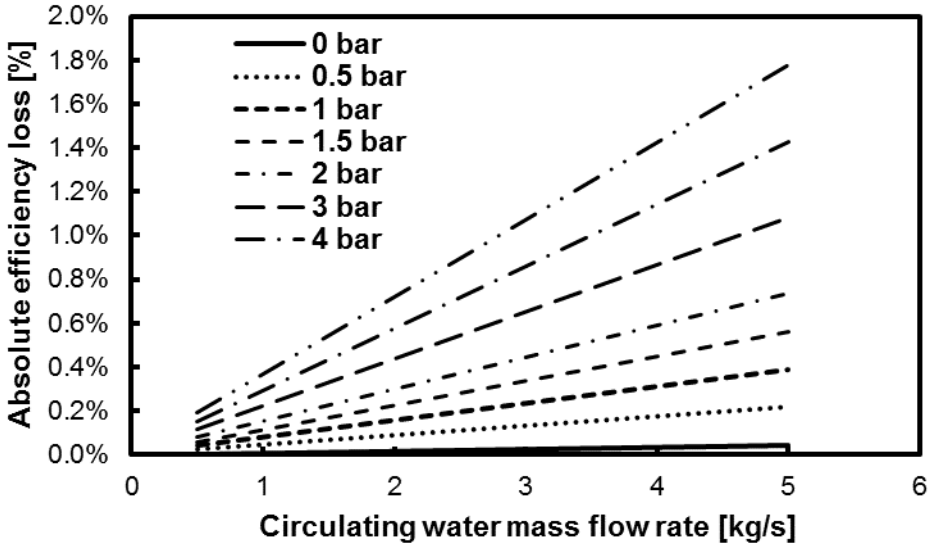

Figure 20: Impact of pump power on final electric efficiency of mGT at water injection mode, expressed as absolute efficiency loss.

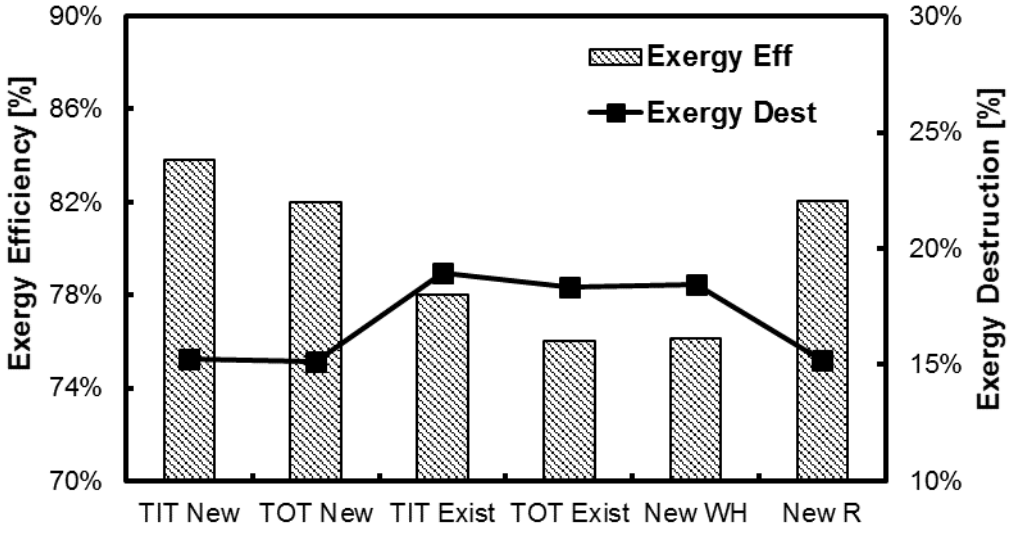

Figure 21: Exergy efficiency and destruction in the heat changer network.

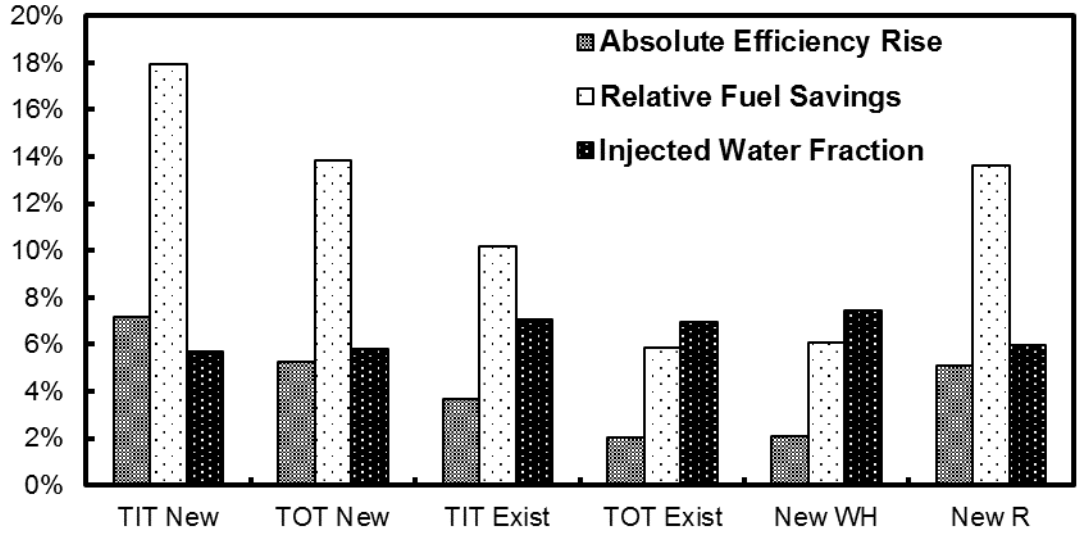

Figure 22: Comparison between the efficiency increase, fuel savings and injected water fraction by introducing water in the mGT.

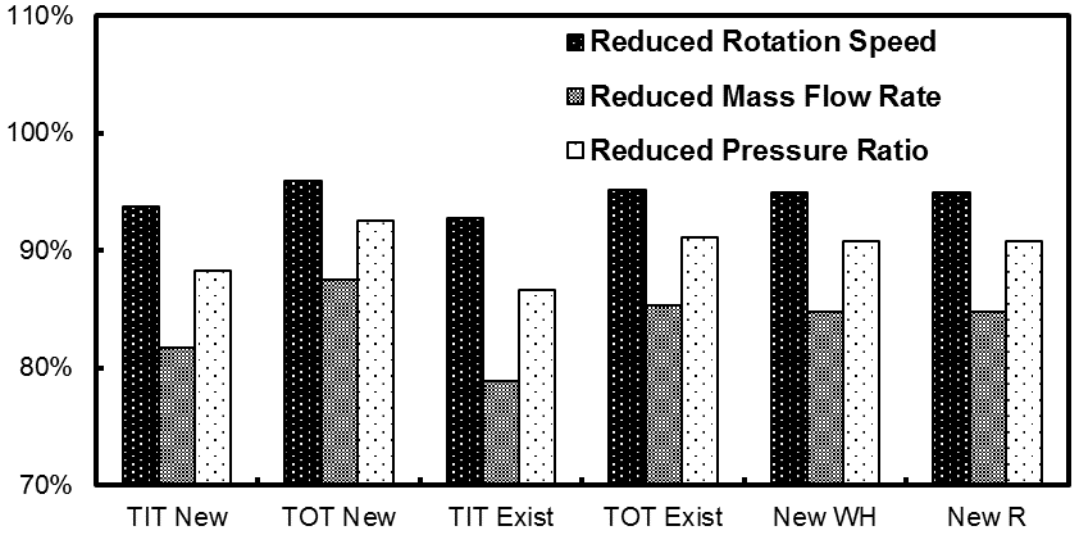

Figure 23: Comparison between the rotation speed, inlet air mass flow rate and pressure ratio reduction by introducing water in the mGT.

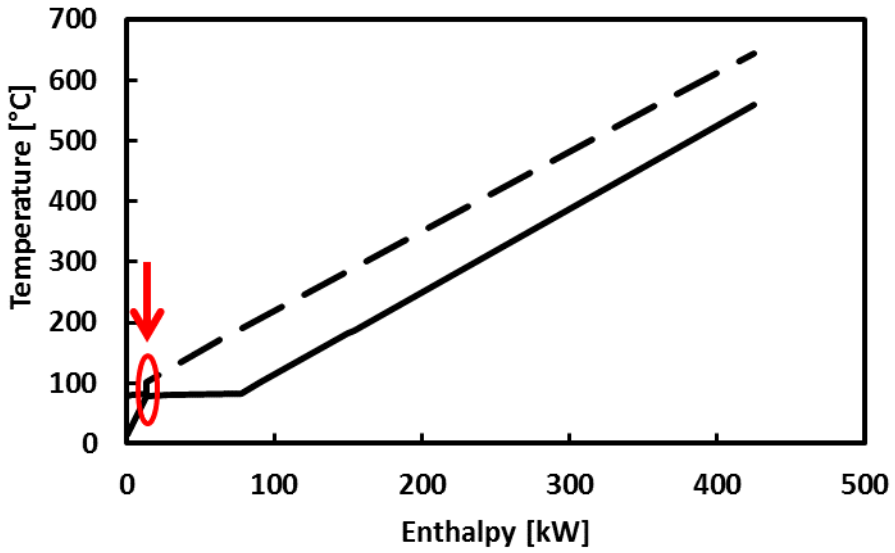

Figure 24: Composite curves of the final layout of the heat exchanger network.

Tables

Table 1: General data about the T100 microturbine.

Electric power	100 kW_e
Thermal power	167 kW_{th}
Electric efficiency	30%
Thermal efficiency	50%
Nominal shaft speed	70,000 rpm

Table 1: Boundary conditions used for the black box heat exchange system.

Compressor	
Pressure ratio	Variable[1]
Isentropic efficiency	0.79
Inlet air temperature	15°C
Turbine	
Turbine back pressure	50 mbar
Isentropic efficiency	0.85
Turbine inlet temperature	950°C
Combustion chamber	
Combustor pressure loss	5%
Heat recovery system	
Hot side pressure loss	3%[2]
Cold side pressure loss	40 mbar
Water injection pressure loss	0.5%
Hot side temperature difference	Variable[3]
Stack temperature	variable
Feed water inlet temperature	15°C
Fuel (methane)	
Fuel temperature	30°C
Fuel pressure	6 bar
LHV	50 MJ/kg

[1] For the simulations of the T100 MGT, generic compressor and turbine maps are used.

[2] The pressure losses of hot and cold side are taken constant and will be a design specification.

[3] For all simulations, the hot side temperature difference and final stack temperature are varied.